Quantum-Classical Dual LSTM Optimization for Internet of Intelligent Vehicles

Muhammad Mustafa Umar Gondel, Uman Khalid, Trung Q. Duong, *Fellow, IEEE*
Een-Kee Hong, *Senior Member, IEEE*, and Hyundong Shin, *Fellow, IEEE*

***Abstract*—The growing complexity of urban transportation networks demands intelligent, data-driven systems capable of real-time perception, optimization, and prediction. Within the Internet of intelligent Vehicles (IoIV), optimal sensor placement is essential for enhancing distributed edge intelligence, as it significantly improves traffic observability, ensures accurate data collection, and enables dynamic decision-making. In this context, we propose a dual approach for hybrid quantum-classical (HQC) optimization—classical for quantum and quantum for classical. First, we formulate the optimal sensor placement problem within the quantum approximate optimization algorithm (QAOA) framework using a minimum vertex cover approach to address its NP-hard nature. Moreover, we enhance the QAOA by integrating long short-term memory (LSTM) networks to adaptively optimize its parameters, thereby achieving faster convergence and improved surveillance coverage in urban transport networks. Second, we employ quantum LSTM (QLSTM) networks to predict traffic flow from data collected by the optimally placed sensors. The QLSTM model reduces the number of learnable parameters while maintaining the expressive capability of classical LSTM architectures. This semantic information is then leveraged to manage traffic flow more effectively, predicting traffic patterns and supporting proactive decision-making. Experimental results demonstrate that the LSTM-guided QAOA outperforms conventional optimization methods such as stochastic gradient descent, achieving faster and more reliable convergence. Likewise, the QLSTM model attains superior predictive accuracy, as evidenced by significant improvements in the explained variance score and root mean squared error. Collectively, these advancements represent a substantial step forward in intelligent traffic management and highlight the practical potential of HQC machine intelligence in IoIV systems.**

***Index Terms*—HQC optimization, IoIV, LSTM networks, optimal sensor deployment, QAOA, QLSTM networks, traffic flow prediction.**

This work was supported by the National Research Foundation of Korea (NRF) grant funded by the Korean government (MSIT) (RS-2025-00556064 and RS-2025-25442355) and by the MSIT (Ministry of Science and ICT), Korea, under the ITRC (Information Technology Research Center) support program (IITP-2026-RS-2021-II212046) supervised by the IITP (Institute for Information & Communications Technology Planning & Evaluation). The work of T. Q. Duong was supported in part by the Canada Excellence Research Chair (CERC) Program CERC-2022-00109, in part by the Natural Sciences and Engineering Research Council of Canada (NSERC) Discovery Grant Program RGPIN-2025-04941, and in part by the NSERC CREATE program (Grant number 596205-2025). *(Corresponding author: Hyundong Shin.)*

M. M. U. Gondel, U. Khalid, E.-K. Hong, and H. Shin are with the Department of Electronics and Information Convergence Engineering, Kyung Hee University, 1732 Deogyeong-daero, Giheung-gu, Yongin-si, Gyeonggi-do 17104 Korea (e-mail: hshin@khu.ac.kr).

T. Q. Duong is with the Faculty of Engineering and Applied Science, Memorial University of Newfoundland, St. John's, NL A1C 5S7, Canada, and is also with the School of Electronics, Electrical Engineering and Computer Science, Queen's University Belfast, Belfast, U.K. (e-mail: tduong@mun.ca).

ACRONYMS

ADAM	Adaptive moment estimation
CNOT	Controlled-NOT
DL	Deep learning
EVS	Explained variance score
GA	Genetic algorithm
GLS	Greedy local search
HQC	Hybrid quantum-classical
IoIV	Internet of intelligent Vehicles
IoT	Internet of Things
LB	Look-back
LSTM	Long short-term memory
MAE	Mean absolute error
MAPE	Mean absolute percentage error
ML	Machine learning
MVC	Minimum vertex cover
NISQ	Noisy intermediate-scale quantum
QAOA	Quantum approximate optimization algorithm
QLSTM	Quantum LSTM
QML	Quantum machine learning
QNN	Quantum neural network
QUBO	Quadratic unconstrained binary optimization
R^2	Coefficient of determination
RMSE	Root mean squared error
SA	Simulated annealing
SGD	Stochastic gradient descent
TOPIS	Transport operation and information service
UTM	Universal transverse mercator
VQA	Variational quantum algorithm
VQC	Variational quantum circuit

I. INTRODUCTION

INTERNET of intelligent Vehicles (IoIV) relies on the optimal sensor placement as a crucial element for the successful deployment of distributed edge intelligence, enhancing traffic observability, ensuring accurate data collection, and enabling dynamic decision-making [1], [2]. By strategically positioning sensors, cities can achieve comprehensive monitoring of traffic conditions and contribute to the development of more resilient and efficient transportation networks. In the context of urban planning and infrastructure management, the deployment of surveillance systems plays a key role in ensuring public safety and monitoring traffic flow. As cities expand and transportation networks become increasingly complex, achieving full surveillance coverage becomes both essential and challenging [3]. To tackle the computational challenges of optimal sensor placement, graph-theoretical approaches

have been widely employed. Urban transport networks can be efficiently modeled as undirected graphs, where crossroads and intersections correspond to vertices and connecting roads to edges [4]. Ensuring comprehensive surveillance over each road segment is equivalent to covering all edges of the graph. Hence, the strategic placement of surveillance cameras at selected intersections aligns with solving the minimum vertex cover (MVC) problem, where a vertex cover is defined as a set of vertices such that each edge is adjacent to at least one vertex in the set. Identifying an optimal MVC ensures that no road segment remains unobserved. However, solving the MVC problem on classical computers becomes NP-hard as the graph size and complexity increase.

Beyond sensor placement, traffic flow prediction from collected data is equally vital for dynamic traffic management in the IoIV. Recent advancements in spatial-temporal models have improved motion prediction accuracy and enabled proactive traffic control [5]–[7]. Optimizing data collection enhances data freshness for reliable analytics, while refined sensor configurations improve data quality [8]–[10]. Adaptive traffic systems also benefit from event-triggered control and occlusion-aware planning, facilitating better decision-making in complex environments [11]–[13]. Furthermore, multimodal sensor fusion and advanced radar-based perception have significantly enhanced traffic monitoring accuracy [14]–[17]. Nevertheless, limitations remain, such as reduced generalizability across diverse urban scenarios, scalability challenges under dynamic traffic conditions, and data integration complexity in heterogeneous sensor networks. Addressing these issues is key to developing more robust, adaptive, and intelligent traffic management systems within IoIV ecosystems.

This paper presents a quantum-classical dual framework that integrates quantum computing, machine learning (ML), and spatial network analysis to address complex optimization and traffic management challenges in intelligent transportation systems. As illustrated in Fig. 1, the framework combines two major components: optimal sensor placement within a road network and traffic flow prediction using data collected from these sensors. The first component constructs detailed road network graphs using OpenStreetMap [18]. This spatial framework streamlines the process of importing, enhancing, and simplifying urban infrastructure data by automating the insertion of intermediate nodes and the consolidation of proximate intersections. This integrated workflow—combining data extraction, node interpolation, and graph simplification—enables efficient generation of spatial network graphs, significantly reducing manual effort and ensuring scalability for large urban areas. In particular, the proposed sensor placement stage is built as a topology-aware and coverage-oriented graph model, where road network geometry, sensing range, and intersection consolidation are incorporated prior to optimization. This design ensures that the formulation remains physically grounded while being amenable to hybrid quantum-classical (HQC) solution methods. The proposed automation facilitates rapid deployment of surveillance network models and supports real-time traffic management applications.

Building upon this spatial foundation, we introduce a HQC optimization framework that integrates quantum computing and classical ML to solve the MVC problem, determining the minimum number and optimal placement of surveillance cameras within transport networks. To enhance the performance of the quantum approximate optimization algorithm (QAOA), we integrate classical long short-term memory (LSTM) networks as adaptive optimizers. The LSTM's ability to retain and leverage long-term dependencies provides a predictive edge, ensuring efficient convergence in the highly complex quantum optimization landscape characterized by high dimensionality and barren plateaus [19]. Further extending this optimization approach, the second component employs quantum LSTM (QLSTM) networks on the strategically placed sensors to advance real-time traffic management. By integrating variational quantum circuits (VQCs), the QLSTM model effectively extracts semantic information from traffic data—including traffic volumes, congestion levels, and vehicle-type distributions—and predicts future traffic patterns for proactive, data-driven traffic control decisions. These predictive insights are transmitted to a central server for further refinement, supporting real-time traffic management strategies. The main contributions of this paper are summarized as follows.

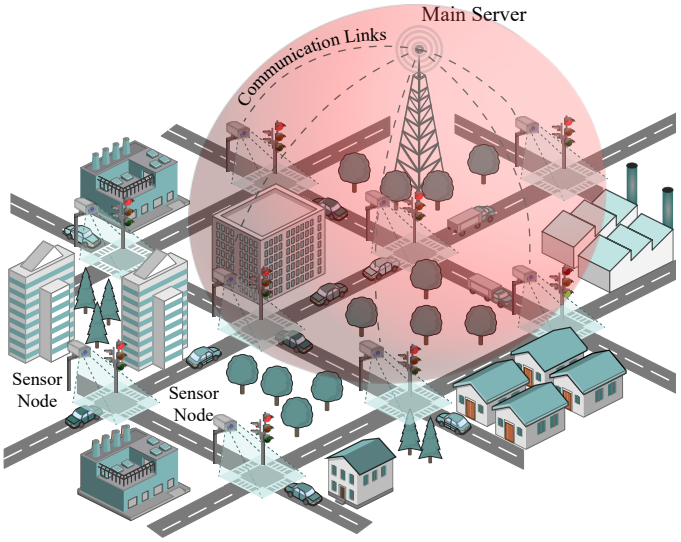

Fig. 1. IoIV depolyment. Optimally placed sensor nodes capture semantic traffic data and communicate with a central server through wireless links. The main server performs decision-making based on the received semantic information and manages real-time traffic control.

- *Automated Spatial Network Construction*: An automated framework is proposed for constructing detailed road network graphs from OpenStreetMap data, incorporating node interpolation and intersection consolidation for efficient surveillance deployment.
- *HQC Sensor Placement Optimization*: The sensor placement problem is mapped to MVC and encoded into QAOA, whose parameters are then optimized using classical LSTM networks to improve convergence efficiency and solution quality in quantum optimization tasks.
- *QLSTM Semantic Traffic Prediction*: The LSTM model is integrated with VQCs to develop a hybrid QLSTM framework that enhances semantic learning. This integration

TABLE I
COMPARATIVE ANALYSIS

Reference	[2]	[20]	[21]	[22]	[23]	[24]	[25]	[26]	[27]	[28]	[29]	[30]	[31]	[32]	Ours
Quantum computing	✗	✗	✗	✗	✗	✓	✓	✓	✗	✓	✓	✓	✓	✓	✓
Sensor optimization	✓	✓	✓	✓	✓	✗	✗	✗	✗	✗	✗	✗	✗	✓	✓
Traffic flow prediction	✗	✗	✗	✗	✗	✗	✗	✗	✓	✓	✗	✓	✗	✗	✓
Real-world data	✗	✗	✗	✓	✓	✗	✓	✓	✓	✓	✗	✓	✓	✗	✓
HQC optimization	✗	✗	✗	✗	✗	✗	✓	✗	✗	✓	✓	✓	✓	✓	✓
Learning-based optimization	✗	✗	✗	✗	✗	✓	✓	✓	✓	✓	✗	✓	✓	✗	✓
Clique problem	✗	✗	✗	✗	✓	✗	✗	✗	✗	✗	✓	✗	✗	✓	✓
Traffic forecasting	✗	✗	✗	✗	✗	∗	∗	∗	✓	✓	✗	✓	∗	✗	✓

Note: ∗ Alternative forecasting

enables effective extraction of latent traffic features, capturing complex spatial-temporal correlations and achieving highly accurate, real-time traffic flow predictions.

- *Experimental Validation*: Comprehensive validation using real-world traffic data from Kyung Hee University (KHU)[1] demonstrates the practical effectiveness of the automated network generation, QAOA optimization, and QLSTM-driven traffic flow prediction in realistic urban environments.

The remainder of this paper is organized as follows. Section II reviews related work. Section III presents the methodology for constructing spatial transportation networks using OpenStreetMap data and introduces the QAOA framework optimized with LSTM networks for solving the MVC problem. Section IV describes the deployment of QLSTM networks for traffic flow prediction, highlighting their integration with VQCs. Section V provides experimental validation using real-world KHU data. Finally, Section VI concludes the paper with a summary.

II. RELATED WORK

Optimal sensor placement plays a pivotal role in transportation engineering by enhancing traffic system observability, improving state estimation accuracy, and enabling effective traffic management. The key challenge lies in balancing comprehensive network coverage with financial and logistical constraints. Previous research has explored diverse strategies to address this issue, including minimizing estimation errors in traffic state estimation [20], leveraging geometric and information-theoretic principles to maximize traffic flow identification [21], [33], exploiting submodularity properties for efficient approximation algorithms [22], and developing exact and heuristic algorithms to generate route sets that balance observability and resilience, achieving near-complete traffic flow estimation with fewer sensors [23]. Accurate travel-time estimation and flow observation further emphasize the importance of strategic sensor deployment. Studies have addressed trade-offs between sensor accuracy and network coverage, considering factors such as sensor failure probabilities [34], GPS-based methodologies for precise sensor placement [35], and comprehensive reviews of sensor placement models [36]. Additionally, approaches for maximizing information gain through optimal sensor deployment [37], integrating multi-sensor data for improved flow reconstruction [38], and tackling flow estimation challenges highlight the complexity and criticality of sensor placement for robust traffic monitoring and management.

HQC algorithms have recently been applied to transportation optimization problems such as routing, scheduling, and traffic management, emphasizing their potential to solve large-scale combinatorial challenges [39]. The vertex cover formulation has been utilized to optimize resource allocation in transport networks, ensuring surveillance coverage with minimal devices. Vertex importance was quantified using the Shapley-Shubik index to enable efficient camera placement and budget distribution across the network [4]. The QAOA has proven effective for solving NP-complete graph optimization problems by efficiently approximating optimal vertex covers, achieving near-optimal solutions with reduced computational complexity compared to classical approaches [29]. The QAOA explores large solution spaces, maintains robustness under noise and hardware constraints, and offers scalability advantages, making it a promising approach for complex optimization tasks in real-world quantum systems [40]. Moreover, quantum combinatorial formulations using quadratic unconstrained binary optimization (QUBO) have provided optimal sensor placement for structural health monitoring, enabling accurate large-scale deployment without model reduction [32].

Traffic forecasting has increasingly focused on leveraging deep learning (DL) and quantum-inspired models to improve prediction accuracy, scalability, and real-time adaptability. Recent surveys have comprehensively examined DL-based models for network traffic prediction, covering architectures ranging from LSTM and convolutional neural networks to graph neural networks and federated learning frameworks [41]. Beyond conventional DL approaches, large language models have also been adapted for traffic forecasting by incorporating spatio-temporal embeddings and graph-based attention mechanisms to capture complex spatial dependencies [42]. Graph-based learning frameworks have enabled dynamic modeling of spatial and temporal dependencies, while adaptive graph construction and meta-learning approaches enhance generalization across heterogeneous traffic networks [27]. Further developments have incorporated hyperbolic embeddings, quantum graph computation, and neural ordinary differential equations to efficiently represent hierarchical road structures and continuous traffic evolution, supporting robust real-time forecasting

[1]Seoul campus.

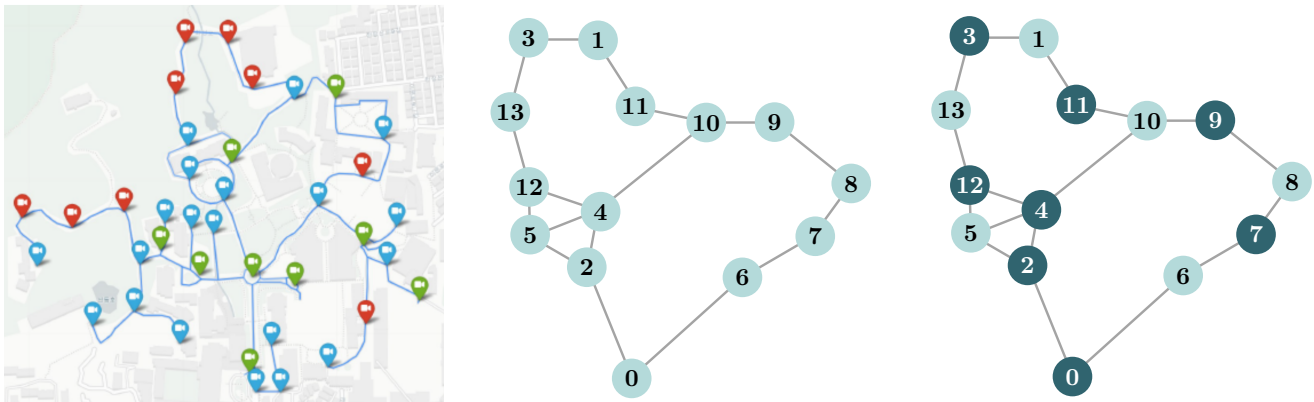

(a) Spatial network construction (b) Graph formulation (c) Graph optimization

Fig. 2. An optimized graph for real-world traffic data: (a) spatial network construction, (b) graph formulation, and (c) graph optimization. The spatial network constructs the road network of KHU (Seoul campus) extracted from OpenStreetMap. Blue markers (nodes) denote intersections and dead ends, while blue lines (edges) represent road segments connecting these nodes. Red markers indicate the insertion of intermediate nodes along graph edges based on a typical sensor range of 80 meters (m). Green markers show the consolidation of proximate intersections into singular nodes by projecting the graph onto an appropriate universal transverse mercator (UTM) zone, setting a tolerance level of 15 m. The graph formulation simplifies the spatial network by selecting 14 nodes for the Hamiltonian formulation. The graph optimization selects 8 nodes for optimal sensor placement, highlighted in a darker shade.

in large-scale IoIV systems [28]. Complementary progress in quantum ML (QML) has demonstrated that quantum neural networks (QNNs) with data re-uploading can capture complex temporal correlations in high-resolution urban traffic data, offering improved expressivity and faster convergence than purely classical models, thereby highlighting the potential of HQC architectures for traffic flow prediction [30].

VQCs serve as the quantum analog of classical neural networks, utilizing parameterized quantum gates to learn complex patterns within data [43], [44]. By optimizing these quantum parameters through iterative training, VQCs can encode richer representations, exploit quantum properties, and have been argued to provide increased representational capacity under specific theoretical assumptions [45], [46]. Quantum models can capture complex temporal dependencies and long-term correlations in sequential data, enabling more accurate and efficient forecasting [25]. A fully quantum implementation of the LSTM cell has replicated classical operations such as addition, multiplication, and activation using quantum gates, demonstrating that QLSTM architectures may achieve exponential speed-up in settings where inputs are processed in quantum superposition and a suitable oracle mechanism is employed to select the desired outcome [47]. The QLSTM model extends the classical LSTM by leveraging the representational power of VQCs to efficiently capture long-term dependencies in temporal data [24]. Previous studies have demonstrated the advantages of QLSTM in various domains, including time-series prediction, solar power forecasting, and indoor localization [26], [48]. More recently, QLSTM-based models have also been integrated into the Internet of Things to enhance predictive analytics in healthcare applications, such as air-quality pollutant prediction for healthy aging and energy expenditure estimation using wearable devices [49], [50].

However, limited research has explored the integration of quantum computing with learning-based frameworks for traffic systems, particularly in addressing the combined challenges of sensor optimization and traffic forecasting. Table I presents a comparative analysis of recent works in this domain, highlighting their scope and methodological focus. While existing works have explored either sensor optimization [2], [20]–[23] or alternative forecasting [24]–[26], [31], few have examined HQC approaches that utilize real-world data for traffic forecasting [27], [28], [30]. Most existing works remain confined to theoretical formulations of quantum algorithms or specific combinatorial problems such as vertex cover [29], [32], offering limited discussion on their practical applicability within IoIV systems. This gap underscores the need for a quantum-enhanced framework that integrates optimization, learning, and real-time forecasting for IoIV.

III. Classical for Quantum: LSTM-QAOA

In this section, we introduce a classical-assisted quantum optimization framework for traffic sensor placement within IoIV systems. The sensor placement stage is formulated as a topology-aware and coverage-oriented graph optimization problem, where the road network is first refined through spatial preprocessing and then represented as an MVC problem on the resulting transportation graph to ensure comprehensive traffic observability with minimal sensors. Given the NP-hard nature of this problem, we employ QAOA to efficiently determine optimal sensor locations. To enhance QAOA's convergence and solution quality, we integrate classical LSTM networks as dynamic optimizers, By leveraging the predictive capability of LSTM, the designed framework guides the selection of QAOA parameters, reducing computational overhead and ensuring efficient sensor deployment in complex traffic networks.

A. Spatial Network Construction

We begin by importing urban infrastructure data from OpenStreetMap [18]. To enhance the resolution of road network graphs, our methodology encompasses two primary phases: i) inserting intermediate nodes along graph edges; and ii) consolidating proximate intersections into singular nodes. The

spatial network graph represents the road topology under consideration for our analysis. Initially, we increase the network's detail by adding nodes at regular intervals along its edges. This process begins with identifying edges that exceed a predefined length threshold. This threshold is determined by the range of sensors used for traffic information extraction. We calculate a series of equidistant points along their length for edges that exceed the threshold length. These points serve as locations for new nodes, effectively subdividing the original edges into shorter segments. Linear interpolation is employed to ensure that the inserted new nodes are precisely positioned along the edge while preserving network integrity and connectivity, as illustrated in Fig. 2(a). This process minimizes deployment costs by reducing the number of required cameras while ensuring that every road segment lies within the surveillance range, thereby improving coverage and monitoring effectiveness of the surveillance network.

After increasing network granularity, the next step focuses on reducing graph complexity by consolidating network nodes. This step is essential for streamlining the network by merging nodes that represent the same physical intersection but appear slightly separated, a common issue stemming from the initial construction of spatial networks from spatial data sources. The consolidation process involves identifying these nodes within a defined proximity and merging them, effectively reducing the total number of nodes and edges in the graph, as shown in Fig. 2(a). This operation not only simplifies the representation of intersections but also preserves the functional navigability of the network, ensuring that the resulting graph remains an accurate abstraction of the real-world road network. Together, these preprocessing steps define the practical modeling layer of the proposed framework, converting raw urban road geometry into a sensing-aware graph representation suitable for coverage optimization.

B. MVC Formulation

Once the spatial network is constructed based on roadway topology, we then determine an optimal strategy for placing sensors on the road network that covers the full range with the minimum number of sensors required to monitor traffic. Under the adopted sensing model, each road segment must be monitored by at least one selected sensing location. Accordingly, edges represent road segments requiring surveillance, while vertices denote candidate sensing nodes after spatial refinement. This provides a compact coverage-oriented graph representation of the deployment problem and motivates a graph-theoretic formulation. This optimal sensor placement problem can be formulated as an MVC problem on the spatial network [51]. In graph theory, a vertex cover $\mathcal{C}$ of an undirected graph $\mathcal{G} = (\mathcal{V}, \mathcal{E})$ is a subset of the vertex set $\mathcal{V}$ such that, for every edge $(i, j) \in \mathcal{E}$, at least one of its endpoints, either i or j, belongs to $\mathcal{C}$. This ensures that every edge in $\mathcal{G}$ is *covered* by at least one of its endpoints included in $\mathcal{C}$. The MVC problem seeks to identify a vertex cover of the smallest possible cardinality within a graph. It is important to note that the graph may possess multiple MVCs solutions of equal minimum size rather than a unique solution.

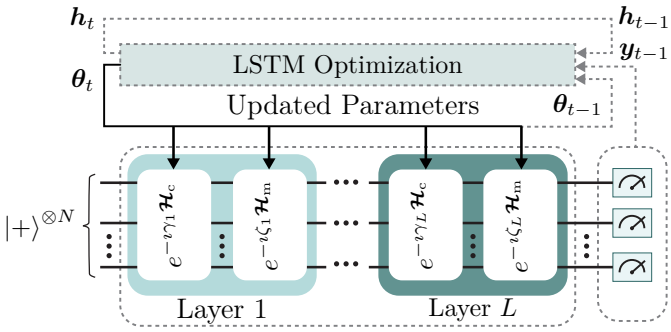

Fig. 3. LSTM-QAOA with circuit depth L and N qubits. This HQC model illustrates a multi-layer QAOA architecture enhanced by LSTM optimization. Starting from the initial quantum state $|+\rangle^{\otimes N}$, the system evolves through L QAOA layers. The ℓth layer consists of two unitary operations $e^{-\imath\gamma_\ell \boldsymbol{\mathcal{H}}_c}$ and $e^{-\imath\zeta_\ell \boldsymbol{\mathcal{H}}_m}$, corresponding to time evolution under the cost Hamiltonian $\boldsymbol{\mathcal{H}}_c$ and the mixer Hamiltonian $\boldsymbol{\mathcal{H}}_m$, parameterized by γ_ℓ and ζ_ℓ, respectively. The variational parameters γ_ℓ and ζ_ℓ, $\ell = 1, 2, \ldots, L$, are updated iteratively by the LSTM optimization module, thereby optimizing the QAOA performance.

Successfully finding any such minimum-size cover provides a valid solution to the MVC problem.

Let $x_j = 1$ if the vertex j is included in the cover and $x_j = 0$ otherwise. The MVC problem can be formulated as the following constrained linear optimization problem [52]:

$$\begin{aligned} \min \quad & \sum_{j \in \mathcal{V}} x_j \\ \text{subject to}: \quad & x_i + x_j \geq 1, \ \forall (i,j) \in \mathcal{E}. \end{aligned} \tag{1}$$

The objective function minimizes the number of vertices in the cover $\mathcal{C}$, while the constraints ensure that for every edge (i, j) in $\mathcal{E}$, at least one of the endpoints of each edge is included in $\mathcal{C}$. We can transform this constrained optimization problem into an unconstrained optimization problem by adding a penalty function for the binary vector $\boldsymbol{x}$ of decision variables x_j [29]:

$$f(\boldsymbol{x}) = a \sum_{(i,j) \in \mathcal{E}} (1 - x_i - x_j + x_i x_j) + b \sum_{j \in \mathcal{V}} x_j \tag{2}$$

where a and b are positive scalar weights chosen such that $0 < b < a$, ensuring that minimizing the penalty (2) is equivalent to solving the original MVC problem. Note that a enforces edge coverage constraints, while b minimizes the total number of selected vertices. This resulting formulation corresponds to a QUBO model. Subsequently, we describe how quantum computers can be used to solve the QUBO problem.

C. QAOA Formulation

Finding an MVC solution on classical computers is NP-hard. In contrast, quantum computers provide alternative approaches that remain effective even when combinatorial optimization problems become computationally prohibitive. The QAOA operates by evolving the initial state of a quantum system through a sequence of parameterized unitary transformations, generated by problem-specific and mixer Hamiltonians [53], thereby yielding a parameterized final quantum state. To solve the MVC problem on quantum computers, we first encode the problem into a Hamiltonian that the quantum system can process. This task involves mapping the MVC

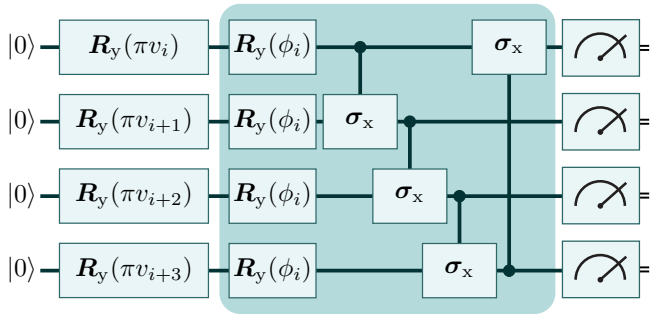

Fig. 4. A single-layered VQC for QLSTM. The circuit consists of a data-encoding layer, a parameterized quantum layer, and measurement operations.

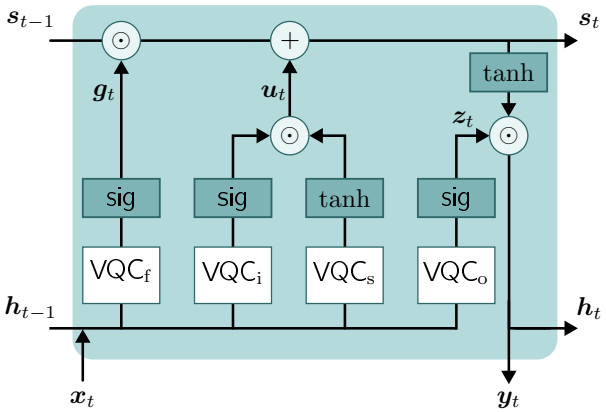

Fig. 5. A QLSTM cell architecture for traffic flow prediction. The $\mathrm{sig}(\cdot)$ and $\tanh(\cdot)$ blocks denote sigmoid and hyperbolic tangent activation functions, respectively. The variables $\boldsymbol{x}_t$, $\boldsymbol{h}_t$, $\boldsymbol{s}_t$, and $\boldsymbol{y}_t$ represent the inputs, hidden states, cell states, and outputs at time t. The symbol $\odot$ denotes element-wise Hadamard multiplication.

formulation to a cost Hamiltonian $\boldsymbol{\mathcal{H}}_{\mathrm{c}}$ whose ground state (i.e., the lowest-energy state) corresponds to an optimal solution of the MVC problem. The cost Hamiltonian for MVC is derived in [29] by

$$\boldsymbol{\mathcal{H}}_{\mathrm{c}} = \frac{a}{4} \sum_{(i,j)\in\mathcal{E}} \boldsymbol{\sigma}_{\mathrm{z}}^{[i]} \boldsymbol{\sigma}_{\mathrm{z}}^{[j]} + \sum_{j\in\mathcal{V}} \left(\frac{1}{2} b - \frac{1}{4} a d_j \right) \boldsymbol{\sigma}_{\mathrm{z}}^{[j]} \tag{3}$$

where $\boldsymbol{\sigma}_{\mathrm{z}}^{[j]}$ denotes the Pauli-z operator $\boldsymbol{\sigma}_{\mathrm{z}} = |0\rangle\langle 0| - |1\rangle\langle 1|$ acting on the qubit associated with vertex j and the parameter d_j represents the degree of vertex j, i.e., the number of edges connected to vertex j. To implement QAOA, the mixer Hamiltonian $\boldsymbol{\mathcal{H}}_{\mathrm{m}}$ is also defined using the Pauli-x operator $\boldsymbol{\sigma}_{\mathrm{x}} = |0\rangle\langle 1| + |1\rangle\langle 0|$ as follows:

$$\boldsymbol{\mathcal{H}}_{\mathrm{m}} = \sum_{j\in\mathcal{V}} \boldsymbol{\sigma}_{\mathrm{x}}^{[j]} \tag{4}$$

where $\boldsymbol{\sigma}_{\mathrm{x}}^{[j]}$ denotes the Pauli-x operator acting on vertex j. Each vertex j in the graph $\mathcal{G} = (\mathcal{V}, \mathcal{E})$ is represented by a single qubit in the quantum system, whose computational basis state ($|0\rangle$ or $|1\rangle$) indicates whether the vertex is included in the vertex cover or not. The QAOA model is an HQC algorithm designed for noisy intermediate-scale quantum (NISQ) devices to optimize an objective function by iteratively updating the variational parameters of the quantum circuit using a classical optimizer. The quality of QAOA solution depends on both the choice of variational parameters and the circuit depth, which together determine the ansatz expressiveness and the optimization effectiveness.

We begin by defining two parameterized unitary operators corresponding to the cost and mixer Hamiltonians:

$$\boldsymbol{U}\left(\boldsymbol{\mathcal{H}}_{\mathrm{c}}, \gamma_\ell\right) = e^{-\imath\gamma_\ell \boldsymbol{\mathcal{H}}_{\mathrm{c}}} \tag{5}$$

$$\boldsymbol{U}\left(\boldsymbol{\mathcal{H}}_{\mathrm{m}}, \zeta_\ell\right) = e^{-\imath\zeta_\ell \boldsymbol{\mathcal{H}}_{\mathrm{m}}} \tag{6}$$

where γ_ℓ and ζ_ℓ, $\ell = 1, 2, \ldots, L$, are variational parameters to be optimized, L denotes the circuit depth, and $\imath = \sqrt{-1}$. Then, the QAOA ansatz with the variational parameter vectors $\boldsymbol{\gamma} = (\gamma_1, \gamma_2, \ldots, \gamma_L)$ and $\boldsymbol{\zeta} = (\zeta_1, \zeta_2, \ldots, \zeta_L)$ is given by

$$\boldsymbol{U}(\boldsymbol{\gamma}, \boldsymbol{\zeta}) = \prod_{\ell=1}^{L} \boldsymbol{U}\left(\boldsymbol{\mathcal{H}}_{\mathrm{m}}, \zeta_\ell\right) \boldsymbol{U}\left(\boldsymbol{\mathcal{H}}_{\mathrm{c}}, \gamma_\ell\right). \tag{7}$$

By encapsulating the complete set of variational parameters as $\boldsymbol{\theta} = (\boldsymbol{\gamma}, \boldsymbol{\zeta})$, the algorithm initializes from the uniform superposition $|+\rangle^{\otimes N}$ over computational-basis states and evolves it into a parameterized quantum state (see Fig. 3):

$$|\boldsymbol{\psi}(\boldsymbol{\theta})\rangle = \boldsymbol{U}(\boldsymbol{\theta}) |+\rangle^{\otimes N} \tag{8}$$

where $\otimes$ denotes the tensor product, $|+\rangle = (|0\rangle + |1\rangle)/\sqrt{2}$ is the Hadamard-basis state, and N denotes the number of qubits. The optimization objective is to minimize the expectation value of the cost Hamiltonian with respect to the parameterized state as follows:

$$C(\boldsymbol{\theta}) = \langle \boldsymbol{\psi}(\boldsymbol{\theta}) | \boldsymbol{\mathcal{H}}_{\mathrm{c}} | \boldsymbol{\psi}(\boldsymbol{\theta}) \rangle . \tag{9}$$

Hence, we obtain the optimal set of parameters as follows:

$$\boldsymbol{\theta}_\star = \arg\min_{\boldsymbol{\theta}} C(\boldsymbol{\theta}) . \tag{10}$$

This minimization is attained by the iterative HQC optimization loop, in which the variational parameters are repeatedly updated to minimize the measured cost associated with the chosen observable.

D. LSTM Optimization for QAOA Parameters

Major challenges in QAOA lie in the efficient optimization of its tunable variational parameters. Initial parameter values play a significant role in finding the optimal QAOA solution, as random initialization often leads to suboptimal local minima solutions. To address this issue, we use the LSTM model to generate informed parameter initialization and update strategies. Instead of directly optimizing the parameters of quantum circuits, the LSTM network is tasked with learning how to update these parameters in a data-driven manner [54]. In this variational quantum algorithm (VQA), the LSTM serves as a black-box controller for optimizing the VQA parameters.

At each iteration t, the LSTM network receives three inputs of information: i) the cost values $\boldsymbol{y}_{t-1} = C(\boldsymbol{\theta_{t-1}})$ obtained in the previous iteration, ii) the set of corresponding parameters $\boldsymbol{\theta}_{t-1}$ used in the quantum circuit, and iii) the hidden states

Fig. 6. Practical applicability demonstration using real-world experimental data. The top panel shows aerial images of all candidate sensor node locations, with the selected optimal nodes highlighted (eight right nodes) as determined by the proposed optimization framework. The bottom panel presents the geographic locations of the currently deployed traffic sensors and representative visual feeds from two sensors used for traffic flow prediction, where Sensor 1 corresponds to branch D-08 and Sensor 2 corresponds to branch F-04 [55].

$\boldsymbol{h}_{t-1}$ carried over from the previous LSTM step. As shown in Fig. 3, the LSTM processes this information with new hidden states $\boldsymbol{h}_t$ and outputs a new set of parameters $\boldsymbol{\theta}_t$, which are then employed in the quantum circuit to obtain the updated cost function $\boldsymbol{y}_t$ [56], [57]. This feedback loop is repeated over multiple iterations, training the LSTM to progressively minimize the cost function through variational parameter updates.

Unlike conventional optimizers such as stochastic gradient descent (SGD) and adaptive moment estimation (ADAM), which update parameters based solely on the current gradient, the LSTM retains hidden states across iterations. Through repeated interaction with quantum circuits, the LSTM develops an implicit understanding of the underlying complex parameter landscape and generates increasingly effective parameter updates without requiring explicit analytical gradients or optimization rules. After obtaining optimal sensor locations through LSTM-QAOA, the HQC dual optimization proceeds to monitor traffic flow, design control policies, and develop new planning strategies by communicating with the server. Specifically, the QLSTM model is employed to extract traffic information, such as vehicle counts and flow dynamics, from the sensor data, in IoIV networks for desired actions to be taken [58].

IV. Quantum for Classical: VQC-LSTM

Once the sensors are optimally placed, we transition to a quantum-assisted classical learning task for traffic flow prediction. Traffic flow data collected from the sensors is processed using QLSTM networks, which integrate VQCs to enhance temporal modeling. In contrast to classical LSTM models, the QLSTM exploits quantum superposition and entanglement to encode rich traffic dynamics while significantly reducing the number of trainable parameters. This hybrid design enables more efficient and accurate traffic flow predictions, thereby supporting proactive traffic management strategies. The extracted semantic information is subsequently transmitted to the central server for real-time inference and decision-making, facilitating adaptive traffic control under dynamically varying traffic conditions.

A. VQC Layers

Qubits possess the distinct capability to exist in a superposition of states, embodying both 0 and 1 simultaneously [59]. This superposition is described mathematically by a complex-value linear combination of basis states, enabling quantum algorithms to explore multiple computational paths in parallel. A single qubit can be expressed as

$$|\psi\rangle = \alpha\,|0\rangle + \beta\,|1\rangle \tag{11}$$

where α and β are complex probability amplitudes such that $|\alpha|^2 + |\beta|^2 = 1$. To process information, quantum gates apply unitary transformations to qubits while preserving reversibility. We utilize parameterized quantum gates to construct trainable VQCs, which enhance temporal feature extraction within the QLSTM cell. As illustrated in Fig. 4, the VQC architecture consists of three key components: i) a data-encoding layer, ii) a parameterized layer, and iii) measurement operations.

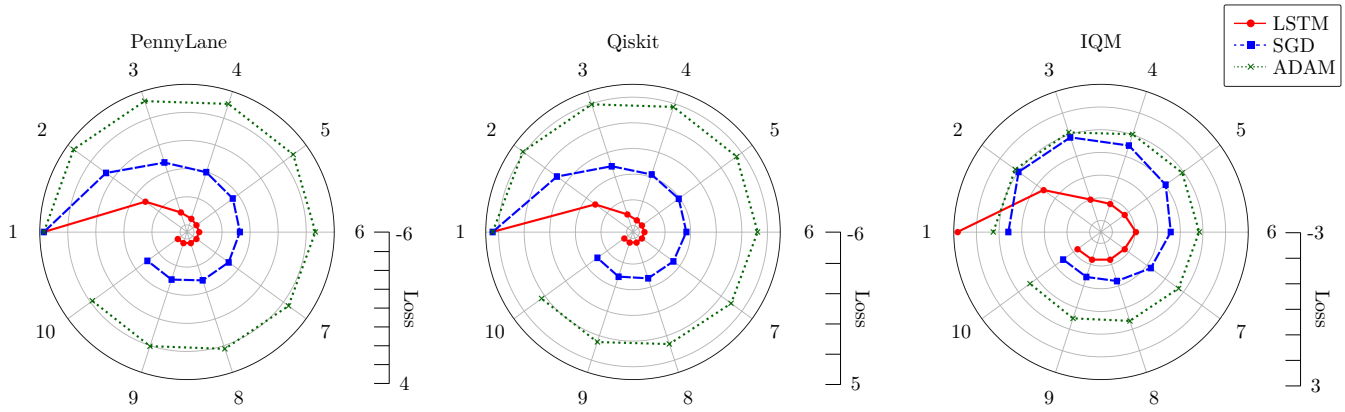

Fig. 7. Average loss as a function of iterations for LSTM, SGD, and ADAM classical optimizers applied to QAOA in solving the MVC problem on the graph Fig. 2(b). Simulation results are plotted across three quantum backends: PennyLane (left), Qiskit (middle), and IQM (right). The LSTM-guided optimizer consistently achieves the lowest loss, demonstrating effective convergence across all platforms.

Let $\boldsymbol{R}_{\mathrm{x}}(\phi)$ and $\boldsymbol{R}_{\mathrm{y}}(\phi)$ be Pauli-x and Pauli-y rotation gates, respectively:

$$\boldsymbol{R}_{\mathrm{x}}(\phi) = e^{-\imath\phi\boldsymbol{\sigma}_{\mathrm{x}}/2} = \begin{bmatrix} \cos\phi/2 & -\imath\sin\phi/2 \\ -\imath\sin\phi/2 & \cos\phi/2 \end{bmatrix} \tag{12}$$

$$\boldsymbol{R}_{\mathrm{y}}(\phi) = e^{-\imath\phi\boldsymbol{\sigma}_{\mathrm{y}}/2} = \begin{bmatrix} \cos\phi/2 & -\sin\phi/2 \\ \sin\phi/2 & \cos\phi/2 \end{bmatrix} \tag{13}$$

where $\boldsymbol{\sigma}_{\mathrm{y}} = \imath\boldsymbol{\sigma}_{\mathrm{x}}\boldsymbol{\sigma}_{\mathrm{z}}$ is the Pauli-y operator. The data-encoding layer initializes qubit states by encoding classical input features v_i into quantum states using the $\boldsymbol{R}_{\mathrm{x}}(\pi v_i)$ rotation gates. Subsequently, the parameterized layer applies additional rotation gates $\boldsymbol{R}_{\mathrm{y}}(\phi_i)$ with trainable parameters ϕ, along with entangling operations using the controlled-NOT (CNOT) gate:

$$\mathsf{CNOT} = |0\rangle\langle 0| \otimes \boldsymbol{I} + |1\rangle\langle 1| \otimes \boldsymbol{\sigma}_{\mathrm{x}} \tag{14}$$

where $\boldsymbol{I}$ denotes the identity operator. These entangling gates enable interaction among qubits, allowing the circuit to capture complex temporal dependencies in the input traffic data.

To retrieve information from the quantum circuit, we perform measurement operations. The probability of observing a measurement outcome is determined by the expectation value of the von Neumann observable, computed as the weighted average of its eigenvalues, with weights given by Born probabilities. This expectation value is given by

$$\langle \boldsymbol{M} \rangle = \langle \psi | \boldsymbol{M} | \psi \rangle \tag{15}$$

where $\boldsymbol{M}$ represents a von Neumann observable, which corresponds to the computational basis in this work. This quantum measurement decodes the qubit information into classical bits, which are subsequently processed within the QLSTM cell.

B. QLSTM Model

The QLSTM model for traffic flow prediction is illustrated in Fig. 5, which extends the classical LSTM by incorporating VQCs to enhance its representational and computational capabilities [24]. In this model, the standard LSTM gates are augmented with VQCs, which are more expressive than classical neural networks. These circuits can potentially provide exponential increases in processing power for specific learning tasks. In the QLSTM cell, the neural network parameters are replaced by VQC operations.

At each time step t, the QLSTM cell receives current inputs $\boldsymbol{x}_t$ as well as previous hidden states $\boldsymbol{h}_{t-1}$ and cell states $\boldsymbol{s}_{t-1}$. The concatenated inputs $\boldsymbol{v}_t = [\boldsymbol{x}_t, \boldsymbol{h}_{t-1}]$ are processed by quantum-enhanced gate mechanisms. Specifically, the forget gate applies VQC transformation $\mathsf{VQC}_{\mathrm{f}}[\boldsymbol{v}_t]$ to these inputs, followed by the sigmoid activation function $\mathsf{sig}(\cdot)$ to determine the forgotten part $\boldsymbol{g}_t$ of the previous cell state. The input gate uses $\mathsf{VQC}_{\mathrm{i}}[\boldsymbol{v}_t]$ and the sigmoid activation to regulate incoming information, which is further modulated by the transformation $\mathsf{VQC}_{\mathrm{s}}[\boldsymbol{v}_t]$ and the hyperbolic tangent activation $\tanh(\cdot)$ to generate candidate cell states $\boldsymbol{u}_t$. The output gate employs another $\mathsf{VQC}_{\mathrm{o}}[\boldsymbol{v}_t]$ followed by the sigmoid activation function to determine the output information $\boldsymbol{z}_t$. These gate operations of the QLSTM cell are represented as follows [24]:

$$\boldsymbol{g}_t = \mathsf{sig}(\mathsf{VQC}_{\mathrm{f}}[\boldsymbol{v}_t]) \tag{16}$$

$$\boldsymbol{u}_t = \mathsf{sig}(\mathsf{VQC}_{\mathrm{i}}[\boldsymbol{v}_t]) \odot \tanh(\mathsf{VQC}_{\mathrm{s}}[\boldsymbol{v}_t]) \tag{17}$$

$$\boldsymbol{z}_t = \mathsf{sig}(\mathsf{VQC}_{\mathrm{o}}[\boldsymbol{v}_t]) \tag{18}$$

where $\odot$ is the element-wise multiplication (Hadamard product). The sigmoid activation function maps input values to the range $[0, 1]$, providing smooth gradients that facilitate stable learning. In contrast, the hyperbolic tangent function maps input values to the range $[-1, 1]$, thereby centering the data and mitigating symmetry issues.

Cell states $\boldsymbol{s}_t$ are updated by combining candidate states and previous cell states modulated by the forget gate. Hidden states $\boldsymbol{h}_t$ are then updated using the output gate and the hyperbolic tangent of updated cell states as follows:

$$\boldsymbol{s}_t = \boldsymbol{u}_t + (\boldsymbol{g}_t \odot \boldsymbol{s}_{t-1}) \tag{19}$$

$$\boldsymbol{h}_t = \boldsymbol{z}_t \odot \tanh(\boldsymbol{s}_t). \tag{20}$$

The outputs $\boldsymbol{y}_t$ of the QLSTM cell at time step t incorporate the improved computational features introduced by quantum operations, thereby enabling efficient processing of sequential traffic data. After T time steps, final outputs $\boldsymbol{y}_T$ encapsulate the extensive information processed throughout the sequence, effectively summarizing the learned temporal dependencies

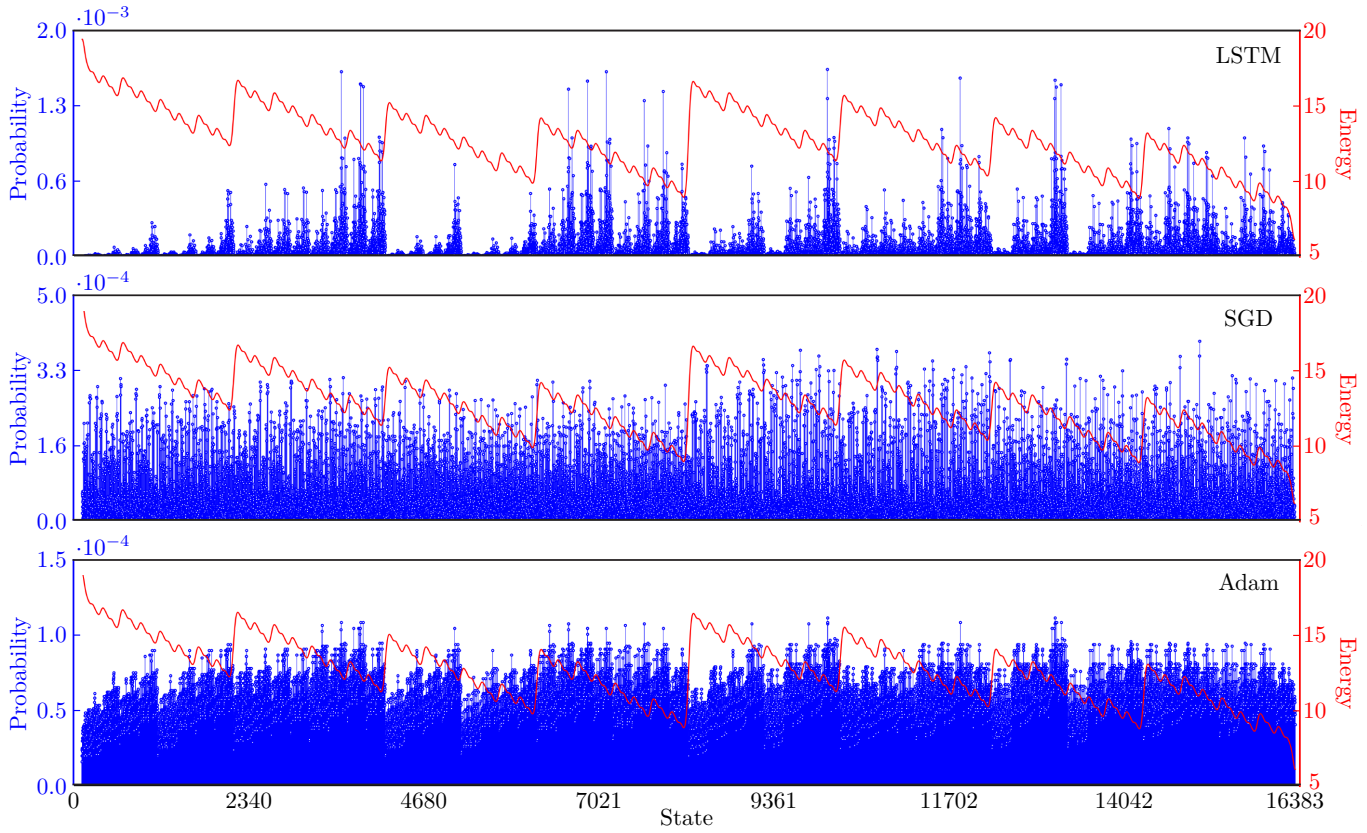

Fig. 8. Solution probability mass (blue) and energy spectra (red) over all computational-basis states for the 14-qubit MVC instance shown in Fig. 2(b). We use PennyLane with LSTM, SGD, and ADAM optimizers.

and semantic features. Once traffic information—such as vehicle counts and flow dynamics—is extracted, the semantic data is transmitted to the server over communication networks for traffic control on the road. The main server then analyzes traffic volumes at intersections of road segments and subsequently performs control actions.

V. Numerical Results

A. Experimental Setup

The effectiveness of the designed optimal sensor placement algorithm is evaluated using real-world traffic data of KHU (Seoul campus), collected from [18]. Real aerial images are provided in the top panel of Fig. 6 to illustrate the physical locations of candidate sensor nodes within KHU. These images depict all feasible sensor deployment points identified on the transportation network, as well as the eight nodes selected by the designed LSTM-QAOA optimization framework. We have validated the LSTM-QAOA framework over three quantum backends—Pennylane, Qiskit and IQM. The algorithm performance is assessed by analyzing sensor deployment within this urban environment and subsequently utilizing data acquired from the optimally placed sensors for traffic flow prediction.

The traffic data used for traffic flow prediction is obtained from the Seoul Transport operation and information service (TOPIS) open traffic information platform provided by the Seoul Metropolitan Government [55]. The dataset consists of vehicle count measurements collected from roadside traffic sensors deployed at various road segments across the city. The bottom panel of Fig. 6 presents traffic sensors deployed in the vicinity of KHU, along with representative visual feeds captured. The left map shows the geographic locations of the sensors, while the middle and right images illustrate sample views from Sensor 1 and Sensor 2, respectively. Sensor 1 and Sensor 2 corresponds to branch D-08 and F-04 in TOPIS dataset, respectively. The data streams obtained from these two sensors are subsequently processed by the QLSTM model to predict traffic flow. We now detail these numerical results, demonstrating both the precision and efficiency of sensor placement and the predictive capabilities of the QLSTM model for traffic flow in the vicinity of KHU.

B. Optimal Sensor Placement

In this example, we set the sensor range to 80 m. To improve the quality and granularity of the spatial graph, additional nodes are inserted at intervals along edges exceeding this sensor range limit. These newly introduced nodes are illustrated as red markers in Fig. 2(a). The spatial network is further simplified by consolidating proximate intersections, indicated by green markers in Fig. 2(a). This step involves projecting the graph onto an appropriate universal transverse mercator (UTM) zone for accurate metric measurements, setting a tolerance level of 15 m to identify nodes in close proximity. This consolidation reduces network complexity while preserving fidelity to the underlying physical road topology.

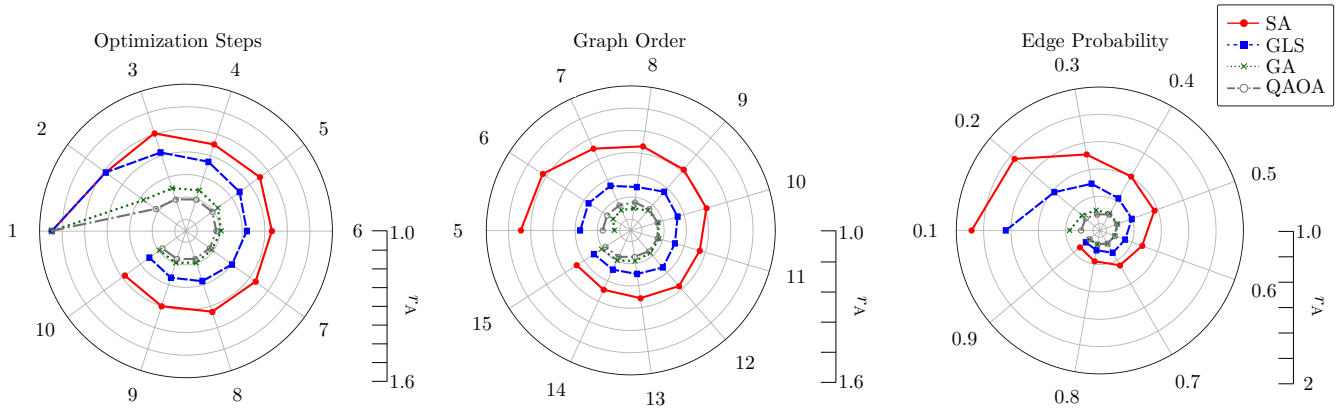

Fig. 9. Approximation ratios r_{A} obtained by LSTM-QAOA and classical metaheuristic algorithms—SA, GLS, and GA—with respect to exact MVC solutions across multiple graph variations. Simulation results are plotted under varying conditions: optimization steps (left), graph order (middle)—increasing nodes from 5 to 15 with a fixed edge probability of $4/7$—and edge probability (right)—increasing from 0.1 to 0.9 with a fixed number of nodes $N = 10$.

For MVC simulations, we select a subgraph of 14 nodes from the graph, as shown in Fig. 2(b). We run simple examples on quantum simulators for demonstration purposes. As quantum hardware with significantly more qubits becomes available, this HQC optimization can be readily extended to large-scale transportation networks. The MVC formulation of the selected graph is cast into the following cost Hamiltonian:

$$\boldsymbol{\mathcal{H}}_{\mathrm{c}} = \frac{5}{4}\sum_{k\in\mathcal{V}_1}\boldsymbol{\sigma}_{\mathrm{z}}^{[k]} + \frac{1}{2}\sum_{\ell\in\mathcal{V}_2\setminus\mathcal{V}_1}\boldsymbol{\sigma}_{\mathrm{z}}^{[\ell]} + \frac{3}{4}\sum_{(i,j)\in\mathcal{V}_3}\boldsymbol{\sigma}_{\mathrm{z}}^{[i]}\boldsymbol{\sigma}_{\mathrm{z}}^{[j]} \quad (21)$$

along with the mixer Hamiltonian

$$\boldsymbol{\mathcal{H}}_{\mathrm{m}} = \sum_{j\in\mathcal{V}_2}\boldsymbol{\sigma}_{\mathrm{z}}^{[j]} \quad (22)$$

where

$$\mathcal{V}_1 = \{2,4,5,10,12\} \quad (23)$$

$$\mathcal{V}_2 = \{0,1,2,3,4,5,6,7,8,9,10,11,12,13\} \quad (24)$$

$$\mathcal{V}_3 = \{(0,2),(0,6),(1,3),(1,11),(2,4),(2,5),(3,13),(4,5),(4,12),(4,10),(5,12),(6,7),(7,8),(8,9),(9,10),(10,11),(12,13)\}. \quad (25)$$

To ascertain the effectiveness of LSTM for QAOA parameter optimization, we compare it with classical optimizers such as SGD and ADAM, as shown in Fig. 7. We run multiple experiments with random initial values and plot average loss values as a function of iterations across three quantum backends: PennyLane, Qiskit, and IQM. We observe that the LSTM optimizer achieves the lowest average loss values compared to SGD and ADAM optimizers. Among the three optimizers, LSTM achieves the fastest convergence, reaching the lowest average loss within fewer iterations compared to both SGD and ADAM across all three quantum backends, as illustrated in Fig. 7. This example reveals that LSTM-QAOA optimization for VQC parameters more often finds the optimal solution for the given MVC problem of optimal sensor placement, achieving a more favorable concentration of probability mass on low-energy states, as illustrated in Fig. 8. In contrast, both SGD and ADAM distribute probability more broadly across the state space, leading to weaker alignment with low-energy optimal solutions. This performance gap highlights the advantage of LSTM in steering the optimization landscape toward lower-energy states. The optimal sensor placement for the 14-node network corresponds to the node set $\{0,2,3,4,7,9,11,12\}$, as illustrated in Fig. 2(c). These nodes ensure comprehensive coverage of the traffic network, enabling effective monitoring and data collection across all critical roadway segments.

Fig. 9 shows a comparative analysis of LSTM-QAOA with three classical metaheuristic algorithms—simulated annealing (SA) [60], greedy local search (GLS) [61], and the genetic algorithm (GA) [62]—demonstrates stable optimization behavior of LSTM-QAOA across the evaluated graph regimes. The dataset is generated from 200 randomized graph instances for each parameter configuration, and the approximation ratio r_{A} is computed relative to the exact MVC solution obtained via an exhaustive brute-force solver as a function of the number of optimization steps, graph order, and edge probability. The ratio r_{A} is defined as the ratio between the size of the vertex cover obtained by a given algorithm and that of the optimal MVC solution, with values closer to unity indicating higher solution quality. We see that LSTM-QAOA consistently achieves approximation ratios closest to unity, indicating solutions that closely approach optimality.

The comparison with classical heuristics illustrates the solution quality obtained by QAOA relative to commonly used classical heuristic approaches under the same problem setting. This comparison provides a practical reference point for evaluating the behavior of the proposed LSTM-guided QAOA framework on the considered MVC instance. As shown in Fig. 9, LSTM-guided QAOA exhibits more stable performance, whereas GA and GLS demonstrate moderate improvements as graph order and edge probability increase. In contrast, SA shows the weakest performance, particularly for limited graph sizes. These results highlight the robustness and effectiveness of the LSTM-guided QAOA optimization strategy when compared with classical heuristic baselines, while serving as a proof-of-concept demonstration of the proposed hybrid optimization framework for NP-hard combinatorial op-

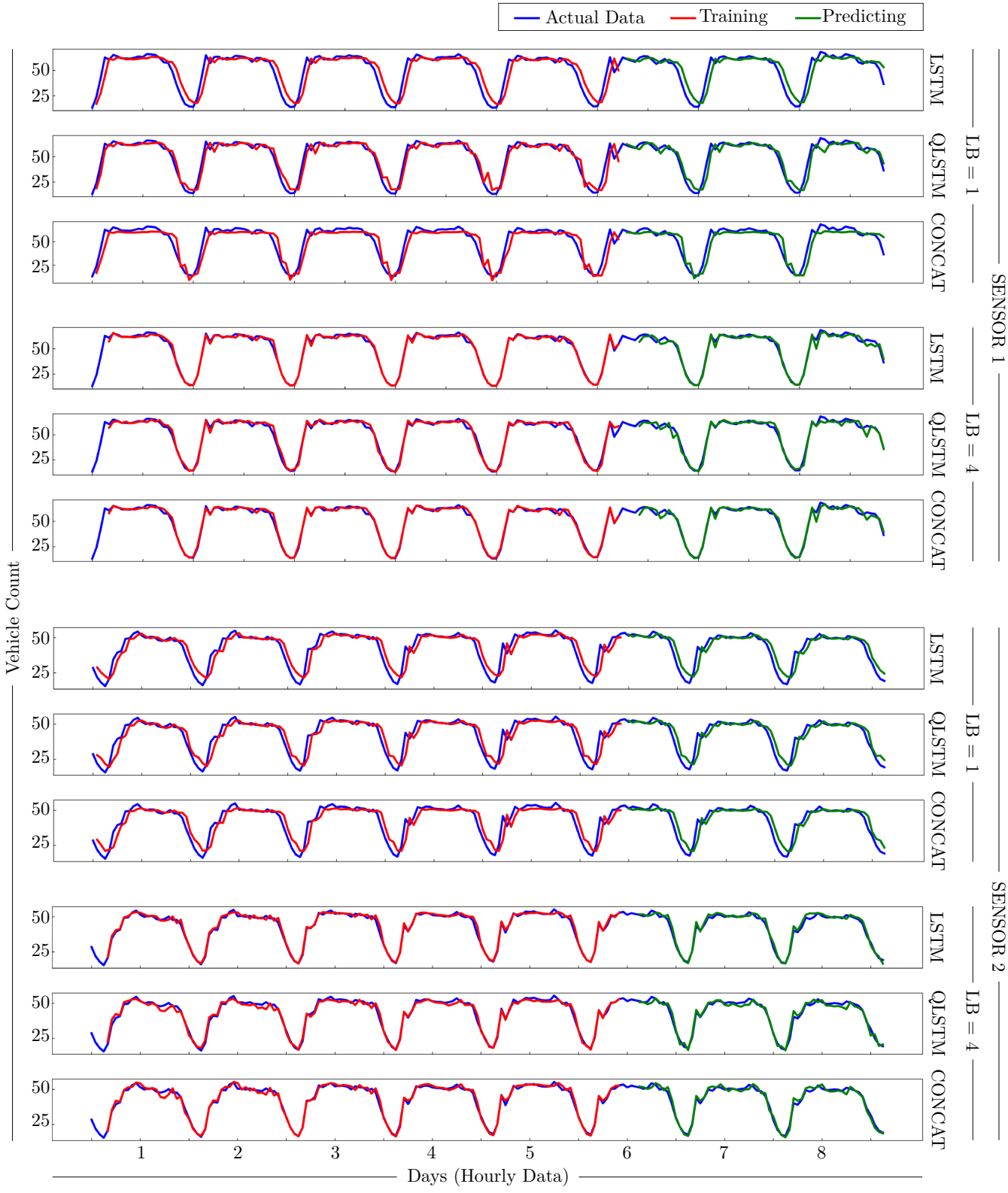

Fig. 10. Training and predicting traffic data for Sensor 1 and Sensor 2 using classical LSTM, QLSTM, and concatenated models when LB = 1 and 4.

TABLE II
PERFORMANCE COMPARISON OF CLASSICAL LSTM, QLSTM, AND CONCATENATED MODELS FOR SENSOR 1 AND SENSOR 2

Sensor	LB	Model	RMSE		MAE		MAPE		R^2		EVS	
			Train	Test	Train	Test	Train	Test	Train	Test	Train	Test
Sensor 1	LB = 1	LSTM	7.842	7.061	5.641	4.964	17.207	14.489	0.801	0.806	0.802	0.808
		QLSTM	**5.578**	**5.566**	**4.133**	**4.187**	**12.743**	**11.327**	**0.899**	**0.879**	**0.901**	**0.880**
		Concatenated	6.951	6.672	5.051	4.779	14.033	12.627	0.844	0.826	0.844	0.827
	LB = 4	LSTM	4.193	4.169	2.382	2.673	6.079	6.165	0.944	0.934	0.944	0.936
		QLSTM	**3.765**	4.133	2.548	2.954	7.120	7.053	**0.954**	0.935	**0.955**	0.938
		Concatenated	3.948	**4.075**	**2.374**	**2.563**	**5.591**	**5.400**	0.951	**0.937**	0.951	**0.939**
Sensor 2	LB = 1	LSTM	5.412	4.726	3.812	3.277	11.561	10.241	0.794	0.828	0.794	0.830
		QLSTM	**5.221**	4.586	**3.679**	**3.195**	**11.301**	**10.094**	**0.808**	**0.839**	**0.808**	**0.841**
		Concatenated	5.316	**4.579**	3.903	3.293	11.636	10.192	0.801	0.839	0.804	0.839
	LB = 4	LSTM	3.386	3.195	2.148	2.180	5.911	5.976	0.919	0.913	0.924	0.925
		QLSTM	**3.077**	**2.810**	1.990	1.967	5.541	5.393	**0.933**	**0.932**	**0.933**	**0.932**
		Concatenated	3.175	3.004	**1.964**	**1.961**	**5.300**	**5.291**	0.929	0.922	0.929	0.923

timization problems. Prior studies have analyzed the scalability of QAOA by examining performance trends as the number of qubits and problem sizes increase, reporting improvements in success probability and favorable time-to-solution scaling for several combinatorial optimization problems [63].

C. Traffic Flow Prediction

Once the sensors are optimally placed, we deploy the VQC-LSTM model on sensor nodes for traffic management, utilizing visual data and vehicle counts to predict traffic patterns. Traffic data are collected through roadside monitoring sensors that continuously record vehicle counts at fixed time intervals. Before training the models, the raw time-series data is preprocessed to ensure consistency and stability during learning. Missing or irregular entries are removed, and the data is normalized to avoid scale-related training issues. The dataset is then divided into training and testing subsets with a ratio of $65 : 35$, while preserving the temporal ordering of observations. To capture temporal dependencies in traffic patterns, sliding windows with different look-back (LB) sizes are applied to construct input sequences for the LSTM and QLSTM models. We employ QLSTM networks to predict traffic flow from time-series data collected from the optimally placed sensors. The extracted traffic information with corresponding timestamps is transmitted to a central server, where predictive models are further refined to inform traffic control strategies. For simulation and analysis, we use real-world traffic data from Seoul, specifically in the vicinity of KHU.

In this example, we employ the QLSTM cell with a 5-qubit quantum layer to process concatenated feature inputs $\boldsymbol{v}_t$. The 5-qubit VQC forms a 25×25 matrix of tunable parameters, effectively replacing the classical weight matrix. This quantum weight matrix allows for more expressive and efficient transformations of the input data. We train and evaluate three models for traffic flow prediction using data collected from optimally placed sensors: classical LSTM [64], QLSTM, and concatenated LSTM models. The classical LSTM consists of standard memory cells designed to capture long-term dependencies in traffic time-series data and contains $10,651$ trainable parameters. In contrast, the QLSTM integrates VQCs to enhance learning efficiency and capture complex temporal patterns, while significantly reducing the number of trainable parameters to 611. The concatenated LSTM model combines both classical LSTM and QLSTM cells into a hybrid architecture with $4,766$ parameters, aiming to balance computational efficiency and predictive performance. For comparison, classical LSTM and QLSTM models are implemented with similar network structures: both employ a hidden size of 50 and include a fully connected linear layer to map the network outputs to the target traffic volumes $\boldsymbol{y}_t$. Specifically, the QLSTM replaces the classical recurrent cell with a quantum-enhanced recurrent cell using a 5-qubit VQC while preserving the same input size, hidden dimension, and output mapping. For the concatenated LSTM architecture, we incorporate the classical LSTM cell with a hidden size of 32 and the QLSTM cell with a hidden size of 10 to evaluate the effectiveness of this hybrid design. All models are trained for $1,000$ epochs using the ADAM optimizer with a learning rate of 0.001 and a batch size of 8. Therefore, the performance difference between the classical LSTM and QLSTM is associated with the change in the recurrent state transition mechanism introduced by the quantum layer.

Fig. 10 compares training and prediction results for Sensor 1 and Sensor 2 using classical LSTM, QLSTM, and concatenated models when two different LB window sizes are set to $\mathrm{LB} = 1$ and $\mathrm{LB} = 4$. In the figure, the actual traffic data (vehicle counts), training data, and model predictions are shown in blue, red, and green, respectively. For both sensors, the QLSTM and concatenated models exhibit closer alignment with the actual traffic data than the classical LSTM model, indicating improved generalization and predictive capability, particularly in capturing sudden traffic fluctuations. Regarding the impact of the LB window size, the models with $\mathrm{LB} = 1$ achieve reasonable performance but show slight limitations in capturing complex temporal dependencies, as evidenced by minor deviations during peak traffic hours. Increasing the window size to $\mathrm{LB} = 4$ enhances prediction accuracy, allowing the models to capture traffic trends more smoothly and reducing discrepancies between actual and predicted data,

particularly during high-traffic periods. The QLSTM model consistently outperforms the classical LSTM, highlighting the benefits of quantum-enhanced learning in modeling nonlinear temporal patterns in traffic flow data.

Table II reports performance metrics—including root mean squared error (RMSE or root MSE), mean absolute error (MAE) [65], mean absolute percentage error (MAPE) [66], coefficient of determination (R^2) [67], and explained variance score (EVS) [68]—for the classical LSTM, QLSTM, and concatenated models evaluated on data from Sensor 1 and Sensor 2 when $\mathrm{LB} = 1$ and 4. These results demonstrate that the QLSTM model outperforms the classical LSTM across all evaluation metrics. For Sensor 1, the QLSTM achieves test RMSE reductions of approximately 21.17% and 0.86% under $\mathrm{LB} = 1$ and $\mathrm{LB} = 4$, respectively, relative to the classical LSTM. For Sensor 2, the corresponding reductions are approximately 2.96% and 12.05%. Beyond RMSE, QLSTM also attains the highest R^2 and EVS under $\mathrm{LB} = 1$, reflecting strong model fit and variance explanation. Increasing the LB window from 1 to 4 significantly improves the performance of the concatenated model across all metrics, highlighting the importance of incorporating longer historical context in capturing complex temporal dependencies. Among the three models, the concatenated model achieves the best performance with an extended LB window, followed by QLSTM, whereas the classical LSTM lags behind. However, this performance gain comes at a cost: the concatenated model requires approximately 8 times more parameters than QLSTM, despite yielding only marginal improvements in predictive accuracy. Notably, even with approximately 17 times more parameters, the classical LSTM still underperforms QLSTM, underscoring the efficiency and effectiveness of HQC optimization for traffic flow prediction. In practical deployments, the proposed framework can operate in a real-time traffic monitoring setting. Once sensors are optimally placed, traffic measurements collected from these sensors can be transmitted to edge computing nodes or centralized servers. The QLSTM model processes incoming time-series data sequentially, allowing the system to continuously update traffic predictions as new observations become available. This capability enables real-time traffic forecasting and supports dynamic traffic management decisions within intelligent transportation systems.

VI. Conclusion

We have presented the HQC optimization framework consisting of two integrated stages: LSTM-QAOA and VQC-LSTM. In the first stage, the LSTM network is utilized to guide the QAOA for solving the MVC problem, enabling optimal sensor placement across transportation networks. The LSTM dynamically adjusts QAOA parameters, achieving faster and more stable convergence, while mitigating barren-plateau limitations that often hinder conventional optimizers. In the second stage, the QLSTM network augmented with VQCs is employed to predict traffic flow using data collected by the optimally deployed sensors. This HQC model effectively captures long-term temporal dependencies, reduces the number of trainable parameters, and improves predictive accuracy compared to classical counterparts. Extensive experiments on real-world traffic data collected from the KHU road network demonstrate that the designed framework delivers both efficient optimization and enhanced forecasting performance. This work advances the integration of quantum computing and LSTM learning architectures, providing a scalable and promising foundation for intelligent data-driven decision-making in IoIV systems.

References

[1] M. Salari, L. Kattan, W. H. K. Lam, H. P. Lo, and M. A. Esfeh, "Optimization of traffic sensor location for complete link flow observability in traffic network considering sensor failure," *Transp. Res. Pt. B-Methodol.*, vol. 121, pp. 216–251, Mar. 2019.

[2] P. Krishnamurthy and F. Khorrami, "Optimal sensor placement for monitoring of spatial networks," *IEEE Trans. Autom. Sci. Eng.*, vol. 15, no. 1, pp. 33–44, Jun. 2018.

[3] U. Khalid, J. ur Rehman, S. N. Paing, H. Jung, T. Q. Duong, and H. Shin, "Quantum network engineering in the NISQ age: Principles, missions, and challenges," *IEEE Netw.*, vol. 38, no. 1, pp. 112–123, Jan. 2024.

[4] V. V. Gusev, "The vertex cover game: Application to transport networks," *Omega*, vol. 97, p. 102102, Dec. 2020.

[5] L. Chu, Z. Hou, J. Jiang, J. Yang, and Y. Zhang, "Spatial-temporal feature extraction and evaluation network for citywide traffic condition prediction," *IEEE Trans. Intell. Veh.*, pp. 1–16, Oct. 2023.

[6] M. Wegener, F. Herrmann, L. Koch, R. Savelsberg, and J. Andert, "Longitudinal vehicle motion prediction in urban settings with traffic light interaction," *IEEE Trans. Intell. Veh.*, vol. 8, no. 1, pp. 204–215, Sep. 2023.

[7] C. Menelaou, S. Timotheou, P. Kolios, C. G. Panayiotou, and M. M. Polycarpou, "Minimizing traffic congestion through continuous-time route reservations with travel time predictions," *IEEE Trans. Intell. Veh.*, vol. 4, no. 1, pp. 141–153, Mar. 2019.

[8] H. Xu, J. Yuan, A. Berres, Y. Shao, C. Wang, W. Li, T. J. LaClair, J. Sanyal, and H. Wang, "A mobile edge computing framework for traffic optimization at urban intersections through cyber-physical integration," *IEEE Trans. Intell. Veh.*, vol. 9, no. 1, pp. 1131–1145, Nov. 2024.

[9] M. Michalopoulou, P. Kolios, C. Panayiotou, and G. Ellinas, "Optimizing vehicles' tracking accuracies while considering information aging," *IEEE Trans. Intell. Veh.*, vol. 8, no. 3, pp. 2538–2550, Aug. 2023.

[10] Y. He, P. Cao, D. Suo, and X. Liu, "A joint optimization of beam distribution and deployment for roadside LiDAR systems to maximize vehicle perception," *IEEE Trans. Intell. Veh.*, pp. 1–15, Jul. 2024.

[11] C. He, D. Sun, M. Zhao, L. Wang, and J. Lin, "CPS-based event-triggered control for connected vehicles with intelligent roadside equipment," *IEEE Trans. Intell. Veh.*, pp. 1–12, Oct. 2023.

[12] C. Zhang, F. Steinhauser, G. Hinz, and A. Knoll, "Occlusion-aware planning for autonomous driving with vehicle-to-everything communication," *IEEE Trans. Intell. Veh.*, vol. 9, no. 1, pp. 1229–1242, Aug. 2024.

[13] L. Guo, H. Chu, J. Ye, B. Gao, and H. Chen, "Hierarchical velocity control considering traffic signal timings for connected vehicles," *IEEE Trans. Intell. Veh.*, vol. 8, no. 2, pp. 1403–1414, Mar. 2023.

[14] C. Creß, W. Zimmer, N. Purschke, B. N. Doan, S. Kirchner, V. Lakshminarasimhan, L. Strand, and A. C. Knoll, "TUMTraf event: Calibration and fusion resulting in a dataset for roadside event-based and RGB cameras," *IEEE Trans. Intell. Veh.*, pp. 1–19, Apr. 2024.

[15] Y. Jin, M. Hoffmann, A. Deligiannis, J.-C. Fuentes-Michel, and M. Vossiek, "Semantic segmentation-based occupancy grid map learning with automotive radar raw data," *IEEE Trans. Intell. Veh.*, vol. 9, no. 1, pp. 216–230, Oct. 2024.

[16] J. Hwang, K.-W. Lim, and D. Kim, "What if vehicles are controlled by the road?" *IEEE Trans. Intell. Veh.*, pp. 1–16, Mar. 2024.

[17] S. Zhou, J. Chen, S. Teng, H. Zhang, and F.-Y. Wang, "Integrating sustainability in future traffic lighting: Designing efficient light systems for vehicle, road, and traffic," *IEEE Trans. Intell. Veh.*, vol. 9, no. 1, pp. 65–68, Nov. 2024.

[18] "OpenStreetMap," 2024. [Online]. Available: https://www.openstreetmap.org/copyright

[19] M. Larocca, S. Thanasilp, S. Wang, K. Sharma, J. Biamonte, P. J. Coles, Łukasz Cincio, J. R. McClean, Z. Holmes, and M. Cerezo, "Barren plateaus in variational quantum computing," *Nat. Rev. Phys.*, vol. 7, no. 4, pp. 174–189, Mar. 2025.

[20] M. Gentili and P. B. Mirchandani, "Locating sensors on traffic networks: Models, challenges and research opportunities," *Transp. Res. Pt. C-Emerg. Technol.*, vol. 24, pp. 227–255, Oct. 2012.

[21] S. A. Nugroho, S. C. Vishnoi, A. F. Taha, C. G. Claudel, and T. Banerjee, "Where should traffic sensors be placed on highways?" *IEEE Trans. Intell. Transp. Syst.*, vol. 23, no. 8, pp. 13 026–13 039, Oct. 2021.

[22] R. Li, N. Mehr, and R. Horowitz, "Submodularity of optimal sensor placement for traffic networks," *Transp. Res. Pt. B-Methodol.*, vol. 171, pp. 29–43, May 2023.

[23] M. Rinaldi and F. Viti, "Exact and approximate route set generation for resilient partial observability in sensor location problems," *Transp. Res. Pt. B-Methodol.*, vol. 105, pp. 86–119, Nov. 2017.

[24] S. Y.-C. Chen, S. Yoo, and Y.-L. L. Fang, "Quantum long short-term memory," in *Proc. IEEE Int. Conf. Acoust., Speech Signal Process. (ICASSP)*, Singapore, Singapore, May 2022, pp. 8622–8626.

[25] Y. Li, Z. Wang, R. Han, S. Shi, J. Li, R. Shang, H. Zheng, G. Zhong, and Y. Gu, "Quantum recurrent neural networks for sequential learning," *Neural Netw.*, vol. 166, pp. 148–161, Sep. 2023.

[26] S. Z. Khan, N. Muzammil, S. M. H. Zaidi, A. J. Aljohani, H. Khan, and S. Ghafoor, "Quantum long short-term memory (QLSTM) vs classical LSTM in time series forecasting: A comparative study in solar power forecasting," *arXiv:2310.17032*, Oct. 2023.

[27] T. Wang, S. Zhao, W. Jia, and D. Shi, "A task-oriented spatial graph structure learning method for traffic forecasting," *IEEE Trans. Intell. Transp. Syst.*, vol. 26, no. 4, p. 4770–4779, Feb. 2025.

[28] M. Rajagopal, R. Sivasakthivel, G. Anitha, K. P. Arunachalam, K. Loganathan, M. Abbas, S. Kalathil, and K. S. Rao, "An efficient intelligent transportation system for traffic flow prediction using meta-temporal hyperbolic quantum graph neural networks," *Sci. Rep.*, vol. 15, no. 1, p. 27476, Jul. 2025.

[29] Y. J. Zhang, X. D. Mu, X.-W. Liu, X. Y. Wang, X. Zhang, K. Li, T. Y. Wu, D. Zhao, and C. Dong, "Applying the quantum approximate optimization algorithm to the minimum vertex cover problem," *Appl. Soft. Comput.*, vol. 118, p. 108554, Mar. 2022.

[30] N. Schetakis, P. Bonfini, N. Alisoltani, K. Blazakis, S. I. Tsintzos, A. Askitopoulos, D. Aghamalyan, P. Fafoutellis, and E. I. Vlahogianni, "Quantum neural networks with data re-uploading for urban traffic time series forecasting," *Sci. Rep.*, vol. 15, no. 1, p. 19400, Jun. 2025.

[31] M. Emu, T. Rahman, S. Choudhury, and K. Salomaa, "Quantum long short-term memory-assisted optimization for efficient vehicle platooning in connected and autonomous systems," *IEEE Open J. Comput. Soc.*, vol. 6, no. 1, p. 119–128, Dec. 2024.

[32] G. San Martín and E. López Droguett, "Quantum-based combinatorial optimization for optimal sensor placement in civil structures," *Struct. Control. Health Monit.*, vol. 2024, no. 1, p. 6681342, Jan. 2024.

[33] E. Castillo, M. Nogal, A. Rivas, and S. Sánchez-Cambronero, "Observability of traffic networks. optimal location of counting and scanning devices," *Transp. Res. Pt. B-Methodol.*, vol. 1, no. 1, pp. 68–102, May 2013.

[34] X. Li and Y. Ouyang, "Reliable sensor deployment for network traffic surveillance," *Transp. Res. Pt. B-Methodol.*, vol. 45, no. 1, pp. 218–231, Jan. 2011.

[35] J. Kianfar and P. Edara, "Optimizing freeway traffic sensor locations by clustering global-positioning-system-derived speed patterns," *IEEE Trans. Intell. Transp. Syst.*, vol. 11, no. 3, pp. 738–747, Jun. 2010.

[36] M. Gentili and P. B. Mirchandani, "Review of optimal sensor location models for travel time estimation," *Transp. Res. Pt. C-Emerg. Technol.*, vol. 90, pp. 74–96, May 2018.

[37] J. Ivanchev, H. Aydt, and A. Knoll, "Information maximizing optimal sensor placement robust against variations of traffic demand based on importance of nodes," *IEEE Trans. Intell. Transp. Syst.*, vol. 17, no. 3, pp. 714–725, Oct. 2015.

[38] E. Lovisari, C. C. D. Wit, and A. Y. Kibangou, "Density/flow reconstruction via heterogeneous sources and optimal sensor placement in road networks," *Transp. Res. Pt. C-Emerg. Technol.*, vol. 69, pp. 451–476, Aug. 2016.

[39] M. Q. Mohammed, H. Meeß, and M. Otte, "Review of the application of quantum annealing-related technologies in transportation optimization," *Quantum Inf. Process.*, vol. 24, no. 9, p. 296, Sep. 2025.

[40] K. Blekos, D. Brand, A. Ceschini, C.-H. Chou, R.-H. Li, K. Pandya, and A. Summer, "A review on quantum approximate optimization algorithm and its variants," *Phys. Rep.-Rev. Sec. Phys. Lett.*, vol. 1068, pp. 1–66, Jun. 2024.

[41] O. Aouedi, V. A. Le, K. Piamrat, and Y. Ji, "Deep learning on network traffic prediction: Recent advances, analysis, and future directions," *ACM Comput. Surv.*, vol. 57, no. 6, pp. 1–37, Feb. 2025.

[42] C. Liu, K. H. Hettige, Q. Xu, C. Long, S. Xiang, G. Cong, Z. Li, and R. Zhao, "ST-LLM+: Graph enhanced spatio-temporal large language models for traffic prediction," *IEEE Trans. Knowl. Data Eng.*, vol. 37, no. 8, pp. 4846–4859, Aug. 2025.

[43] S. Tariq, U. Khalid, B. E. Arfeto, T. Q. Duong, and H. Shin, "Integrating sustainable big AI: Quantum anonymous semantic broadcast," *IEEE Wireless Commun.*, vol. 31, no. 3, pp. 86–99, Jun. 2024.

[44] U. Khalid, M. S. Ulum, M. Z. Win, and H. Shin, "Integrated satellite-ground variational quantum sensing networks," *IEEE Commun. Mag.*, vol. 62, no. 10, pp. 20–27, Oct. 2024.

[45] S. Khairy, R. Shaydulin, L. Cincio, Y. Alexeev, and P. Balaprakash, "Learning to optimize variational quantum circuits to solve combinatorial problems," in *Proceedings of the AAAI Conference on Artificial Intelligence*, vol. 34, no. 03, New York, New York, USA, Feb. 2020, pp. 2367–2375.

[46] M. S. Ulum, U. Khalid, J. W. Setiawan, T. Q. Duong, M. Z. Win, and H. Shin, "Variational anonymous quantum sensing," *IEEE J. Sel. Areas Commun.*, vol. 42, no. 9, pp. 2275–2291, Sep. 2024.

[47] A. Ceschini, A. Rosato, and M. Panella, "Design of an LSTM cell on a quantum hardware," *IEEE Trans. Circuits Syst. II-Express Briefs*, vol. 69, no. 3, pp. 1822–1826, Nov. 2021.

[48] S. Chien, D. Chieng, S. Y. Chen, C. C. Zarakovitis, H. Lim, and Y. Xu, "Applying hybrid quantum LSTM for indoor localization based on RSSI," in *Proc. IEEE Int. Conf. Acoust., Speech Signal Process. (ICASSP)*, Apr. 2024, pp. 131–135.

[49] F. Naz, M. Fahim, A. A. Cheema, B. D. E. Mcniven, T.-V. Cao, R. Hunter, and T. Q. Duong, "Air quality and healthy ageing: Predictive modeling of pollutants using CNN quantum-LSTM," *IEEE Access*, vol. 13, pp. 94 212–94 223, May 2025.

[50] B.-N. D. Tran, M. Fahim, B. D. E. McNiven, M. Guizani, H. Shin, and T. Q. Duong, "Quantum LSTM model for estimation of energy expenditure in human aging using wearable IoT healthcare technology," *IEEE Internet Things J.*, vol. 12, no. 22, pp. 46 051–46 064, Nov. 2025.

[51] R. M. Karp, "Reducibility among combinatorial problems," in *Complexity of Computer Computations*, ser. The IBM Research Symposia Series, R. E. Miller, J. W. Thatcher, and J. D. Bohlinger, Eds. Boston, MA: Springer, 1972.

[52] V. V. Vazirani, "Set cover," in *Approximation Algorithms*. Berlin, Heidelberg: Springer, 2003.

[53] E. Farhi, J. Goldstone, and S. Gutmann, "A quantum approximate optimization algorithm," *arXiv:1411.4028*, Nov. 2014.

[54] G. Verdon, M. Broughton, J. R. McClean, K. J. Sung, R. Babbush, Z. Jiang, H. Neven, and M. Mohseni, "Learning to learn with quantum neural networks via classical neural networks," *arXiv:1907.05415*, Jul. 2019.

[55] Seoul Metropolitan Government, "Seoul transport operation and information service (TOPIS) - traffic information," 2023. [Online]. Available: https://topis.seoul.go.kr/openMain.do

[56] D. E. Rumelhart, G. E. Hinton, and R. J. Williams, "Learning internal representations by error propagation," *Biometrika*, vol. 71, no. 1, pp. 599–607, Sep. 1986.

[57] R. S. Sutton, "Learning to predict by the methods of temporal differences," *Mach. Learn.*, vol. 3, pp. 9–44, Aug. 1988.

[58] U. Khalid, M. S. Ulum, A. Farooq, T. Q. Duong, O. A. Dobre, and H. Shin, "Quantum semantic communications for metaverse: Principles and challenges," *IEEE Wireless Commun.*, vol. 30, no. 4, pp. 26–36, Aug. 2023.

[59] M. A. Nielsen and I. L. Chuang, *Quantum computation and quantum information*. Cambridge university press, 2010.

[60] S. Kirkpatrick, C. D. Gelatt Jr, and M. P. Vecchi, "Optimization by simulated annealing," *Science*, vol. 220, no. 4598, pp. 671–680, May 1983.

[61] M. M. Halldórsson, "Approximations of independent sets in graphs," in *Approximation Algorithms for Combinatorial Optimization*, Berlin, Germany, Jan. 2006, pp. 1–13.

[62] D. E. Goldberg, "Genetic algorithm in search, optimization and machine learning, addison," *Wesley Publishing Company, Reading, MA*, vol. 1, no. 98, p. 9, 1989.

[63] J. Montanez-Barrera and K. Michielsen, "Toward a linear-ramp QAOA protocol: evidence of a scaling advantage in solving some combinatorial optimization problems," *npj Quantum Inform.*, vol. 11, no. 1, p. 131, Aug. 2025.

[64] H. Sak, A. W. Senior, and F. Beaufays, "Long short-term memory based recurrent neural network architectures for large vocabulary speech recognition," *arXiv:1402.1128*, Feb. 2014.

[65] C. J. Willmott and K. Matsuura, "Advantages of the mean absolute error (MAE) over the root mean square error (RMSE) in assessing average model performance," *Clim. Res.*, vol. 30, no. 1, pp. 79–82, Dec. 2005.
[66] A. D. Myttenaere, B. Golden, B. L. Grand, and F. Rossi, "Mean absolute percentage error for regression models," *Neurocomputing*, vol. 192, pp. 38–48, Jun. 2016.
[67] J. O. Rawlings, S. G. Pantula, and D. A. Dickey, *Applied Regression Analysis: A Research Tool*, 2nd ed., ser. Springer Texts in Statistics. Springer, New York, NY, Apr. 1998.
[68] T. Hastie, J. Friedman, and R. Tibshirani, *The Elements of Statistical Learning: Data Mining, Inference, and Prediction*, 1st ed., ser. Springer Series in Statistics. Springer, New York, NY, Nov. 2001.

Muhammad Mustafa Umar Gondel received his B.S. degree in Electrical Engineering from the National University of Sciences and Technology (NUST) , Islamabad, Pakistan, in 2021. He is currently pursuing Ph.D. in Electronics Engineering from Kyung Hee University (KHU), South Korea.

His research interests include quantum computing, quantum machine learning, and wireless communications.

Uman Khalid received his B.S. degree in Electronics Engineering from the Ghulam Ishaq Khan (GIK) Institute, Topi, Pakistan, in 2015, and his Ph.D. in Electronics Engineering from Kyung Hee University, South Korea, in Feb. 2023. Currently, he is a Research Professor with the Department of Electronics and Information Convergence Engineering, Kyung Hee University, South Korea. Before joining as a Research Professor, he served as a Postdoctoral Fellow with the same department from Mar. 2023 to Feb. 2026. His research interests include quantum information science, quantum semantic communications, and quantum networks.

Trung Q. Duong (Fellow, IEEE) is currently a Canada Excellence Research Chair (CERC) and a Full Professor with Memorial University, St. John's, NL, Canada. He is also an Adjunct Professor with Queen's University Belfast, Belfast, U.K., and Kyung Hee University, Yongin-si, South Korea. From 2017 to 2019, he was a Distinguished Advisory Professor with Inje University, Gimhae, South Korea. His research interests include wireless communications, quantum machine learning, and quantum optimization.

Dr. Duong was an Editor/Guest Editor of the IEEE TRANSACTIONS ON WIRELESS COMMUNICATIONS, IEEE TRANSACTIONS ON COMMUNICATIONS, IEEE TRANSACTIONS ON VEHICULAR TECHNOLOGY, IEEE TRANSACTIONS ON NETWORK SCIENCE AND ENGINEERING, IEEE COMMUNICATIONS LETTERS, IEEE WIRELESS COMMUNICATIONS LETTERS, IEEE WIRELESS COMMUNICATIONS, IEEE COMMUNICATIONS MAGAZINES, IEEE NETWORK, and IEEE JOURNAL ON SELECTED AREAS IN COMMUNICATIONS. He is the Editor-in-Chief of IEEE COMMUNICATIONS SURVEYS & TUTORIALS and an IEEE ComSoc Distinguished Lecturer. He was the recipient of the Best Paper Award at the IEEE VTC-SPRING 2013, IEEE ICC 2014, IEEE GLOBECOM 2016, 2019, 2022, IEEE DSP 2017, IWCMC 2019, 2023, and 2024, and IEEE CAMAD 2023, 2024. He received two prestigious awards from the Royal Academy of Engineering (RAEng): RAEng Research Chair and the RAEng Research Fellow, and the prestigious Newton Prize 2017. He is also a fellow of the Engineering Institute of Canada (EIC), Canadian Academy of Engineering (CAE), Institution of Engineering and Technology (IET), and Asia-Pacific Artificial Intelligence Association (AAIA).

Een-Kee Hong (Senior Member, IEEE) received the B.S., M.S., and Ph.D. degrees in electrical engineering from Yonsei University, in 1989, 1991, and 1995, respectively. He was a Senior Research Engineer at SK Telecom, from September 1995 to February 1999, and a Visiting Senior Engineer at NTT DoCoMo, from October 1997 to December 1998. From 2006 to 2007, he was a Visiting Professor at Oregon State University. Since 1999, he has been a Professor and the Vice Dean of the College of Electronics and Information Engineering, Kyung Hee University, South Korea. His research interests include physical layer in wireless communication, radio resource management, and spectrum engineering. He received the Best Paper Award, the Institute of Information Technology Assessment, and the Haedong Best Paper Award, KICS; and the Order of Merit of the Republic of Korea for his contribution to information and communication.

Hyundong Shin (Fellow, IEEE) received the B.S. degree in Electronics Engineering from Kyung Hee University (KHU), Yongin-si, Korea, in 1999, and the M.S. and Ph.D. degrees in Electrical Engineering from Seoul National University, Seoul, Korea, in 2001 and 2004, respectively. During his postdoctoral research at the Massachusetts Institute of Technology (MIT) from 2004 to 2006, he was with the Laboratory for Information Decision Systems (LIDS). In 2006, he joined the KHU, where he is now the Dean of the College of Electronics & Information as well as the College of Software. His research interests include quantum information science, wireless communication, and machine intelligence. Dr. Shin received the IEEE Communications Society's Guglielmo Marconi Prize Paper Award and William R. Bennett Prize Paper Award. He served as the Publicity Co-Chair for the IEEE PIMRC and the Technical Program Co-Chair for the IEEE WCNC and the IEEE GLOBECOM. He was an Editor of IEEE TRANSACTIONS ON WIRELESS COMMUNICATIONS and IEEE COMMUNICATIONS LETTERS.